Supporting Information

α-Aminoisobutyric Acid Stabilized Peptide SAMs with low Nonspecific Protein Adsorption and Resistance Against Marine Biofouling.

Cindy D. Beyer,[†] [‡] Matthew L. Reback,[§] [‡] Srinivasa M. Gopal,[ǂ] Kim A. Nolte, [†] John A. Finlay, [⊥] Anthony S. Clare, [⊥] Lars V. Schäfer, [ǂ] Nils Metzler-Nolte,[§] Axel Rosenhahn[†*]*

[†]Analytical Chemistry – Biointerfaces, [§]Inorganic Chemistry I – Bioinorganic Chemistry, [ǂ]Theoretical Chemistry, Ruhr University Bochum, 44801 Bochum, Germany

[⊥]School of Natural and Environmental Science, Newcastle University, Newcastle upon Tyne NE1 7RU, UK

Number of pages: 8

Number of figures: 8 (Figures S1-S8)

Number of tables: 1 (Table S1)

Table of Contents

1) Molecular Dynamics Simulations

Peptides SG, SG^{2Aib} and SQ^{2Aib} with 11-(acetylthiol)undecanoyl (C10 spacer) attached to the N-terminus were simulated in explicit water and ethanol. The Amber ff99SB-ILDN[1,2] force field was used for the peptides. The generalized Amber force field (GAFF)[3] with AM1-BCC charges[4] was used for the C10 spacer. Water was represented by the TIP3P model.[5] For ethanol, a GAFF-based generic organic solvents force field [6] was used, and parameters for Aib were obtained from REDDB database.[7] For each peptide, two independent simulations starting from i) an extended, (ii) a helical structure were performed in both water and ethanol for 2.5 μs each, to remove any bias due to the starting structure and to check convergence of the MD simulations.

All simulations were run under NPT conditions at 298 K and 1bar using a leap-frog integrator with a 2 fs time step. Constant temperature and pressure were achieved using a velocity rescaling thermostat[8] and Berendsen barostat[9], respectively. The SETTLE[10] and LINCS[11] constraint algorithms were used. The short range Lenard-Jones and electrostatic interactions were truncated at 1.0 nm and the long range electrostatics were handled with the smooth particle-mesh Ewald (PME) scheme.[12] An analytical dispersion correction for energy and pressure was applied to compensate for the truncation of the Lennard-Jones interactions. All simulations and analyses were done with Gromacs Version 5.1.2[13]

A total of 12 simulations (of 2.5 μs each) were performed. The final analysis was done on the individual as well as combined trajectories from the independent simulations. The end-to-end distances (peptide C- to N-terminus) were calculated after discarding the first 100 ns. The distribution of the end-to-end distance was found to be almost identical irrespective of the starting structure.

2) Calculation of packing density

The extended zigzag length of each peptide was calculated using the standard distance of 3.5 Å per amino acid. The 11-mercaptoundecanioc acid (C10 spacer) and dodecanethiol (DDT) both have a length of ≈ 1.5 nm. The total length of the peptide plus the C10 spacer (assuming extended zigzag conformation) is the number of amino acids multiplied by 3.5 Å plus the length of the spacer of 1.5 nm. To obtain an indicator of the packing density we first normalized the experimental DDT film thickness d_{exp} to the theoretical length of the DDT molecule of $d_{the} \approx 1.5$ nm (which corresponds to a packing density of 92% if a tilting angle of 30° with respect to the surface normal is assumed). The relative packing densities (ρ) of the peptide + C10 spacer SAMs were then calculated in comparison to a densely packed aliphatic DDT SAM:

$$\rho = \frac{\frac{d_{exp}}{d_{the}}}{\frac{d_{exp(DDT)}}{d_{the(DDT)}}} \qquad \text{eq. 1}$$

Example calculation for SG SAM ($S(CH_2)_{10}C(O)$(SGKGSSGSS)

Theoretical thickness: (9 x 3.5 Å) + 15.3 Å = 46.8 Å (4.68 nm)

Experimental thickness: 2.49 nm

Relative packing density compared to DDT: ρ =0.73 (73%)

3) **ATR Spectral data**

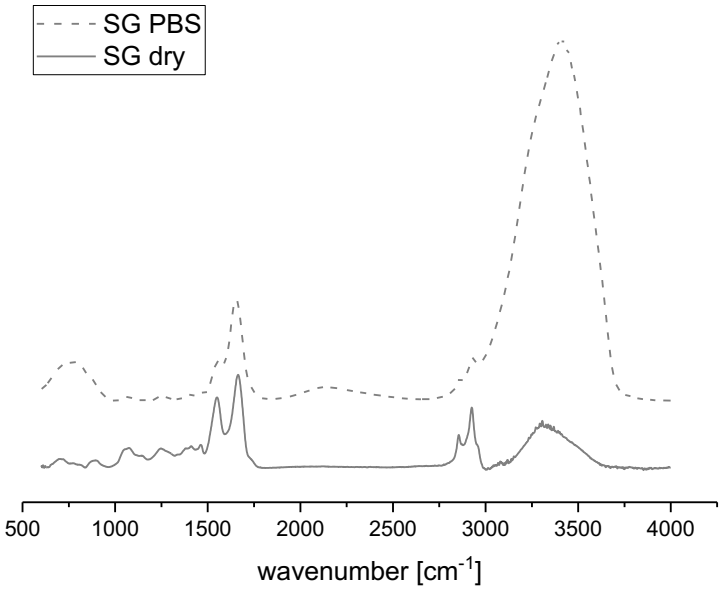

Figure S1 IR spectra of peptide surface SG in dry state and with PBS.

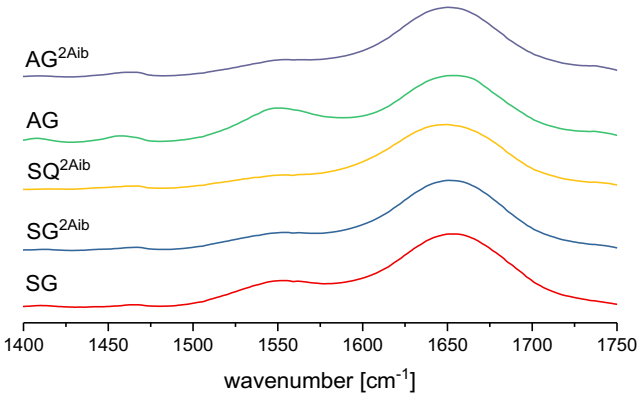

Figure S2 Amid I peaks of peptide SG, SG^{2Aib}, SQ^{2Aib}, AG, AG^{2Aib}.

4) Enzymatic degradation resistance determined by HPLC

For the assay 0.1 mg/mL enzyme was dissolved in TRIS-puffer (pH=7.4) and 1.0 mg/mL of used peptide was dissolved in (20/80) v% acetonitrile/H_2O. 20 μL of enzyme were added to this peptide solution and stored for 1, 2, 3 and 4 h in a heating block at a temperature of 30°C. After the indicated reaction time, 15 μL of enzyme/peptide solution was injected into an HPLC (Knauer Smartline System) by using reversed-phase C18 column. The eluents Millipore water and MeCN contains 0.1 % TFA. The runs were carried out with a flow rate of 1.0 mL/min and

a linear gradient of A (95 v% millipores water, 5 v% MeCN, 0.1 v%TFA) and B (5 v% millipores water, 95 v% MeCN, 0.1 v% TFA). The spectra were detected by UV at 254 nm under ambient temperature.

Table S1 Peak areas of HPLC chromatogram after 1h, 2h, 3h, and 4h enzymatic degradation with trypsin.

	2018/09/19	2018/12/11	2018/12/12
time [h]	SG [peak area]		
1	0.09725	0.09725	0.08079
2	0.05588	0.05588	0.02411
3	0.02469	0.02469	0.00647
4	0.01328	0.01328	0.00517

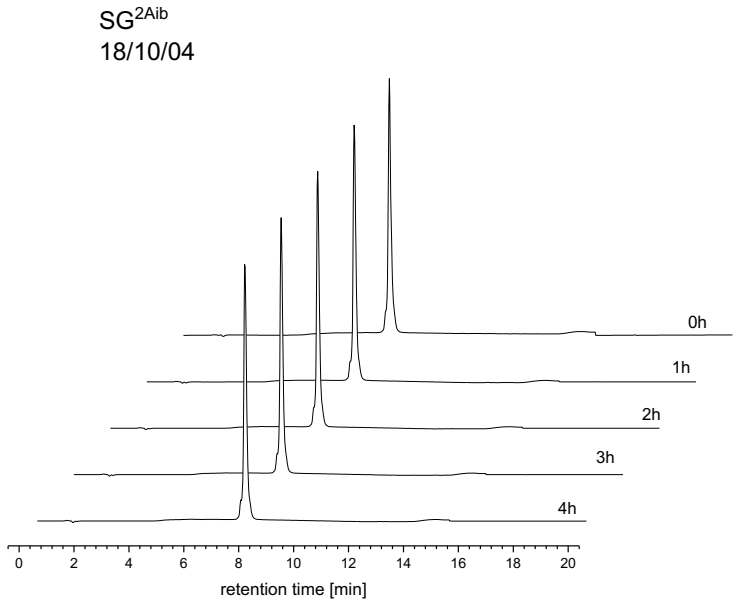

Figure S3 Chromatograms of enzymatic degradation after 1, 2, 3 and 4h with trypsin from peptide SG^{2Aib}.

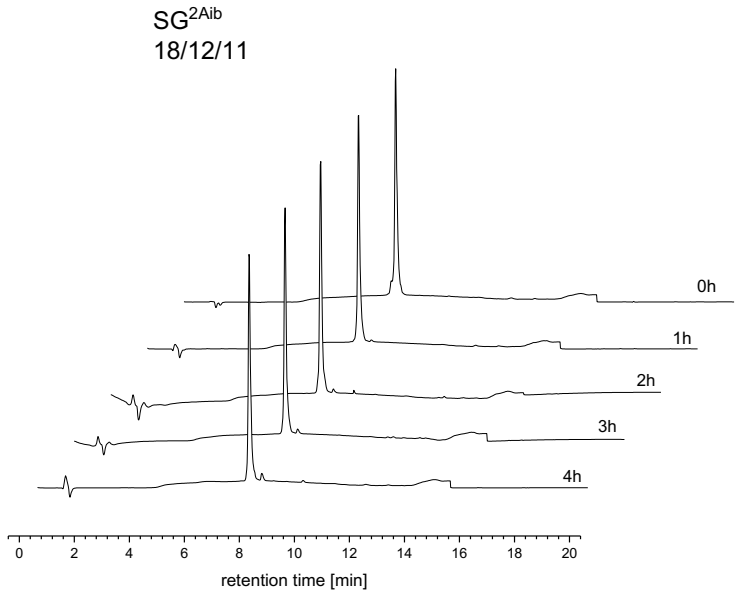

Figure S4 Chromatograms of enzymatic degradation after 1, 2, 3 and 4h with trypsin from peptide SG^{2Aib}.

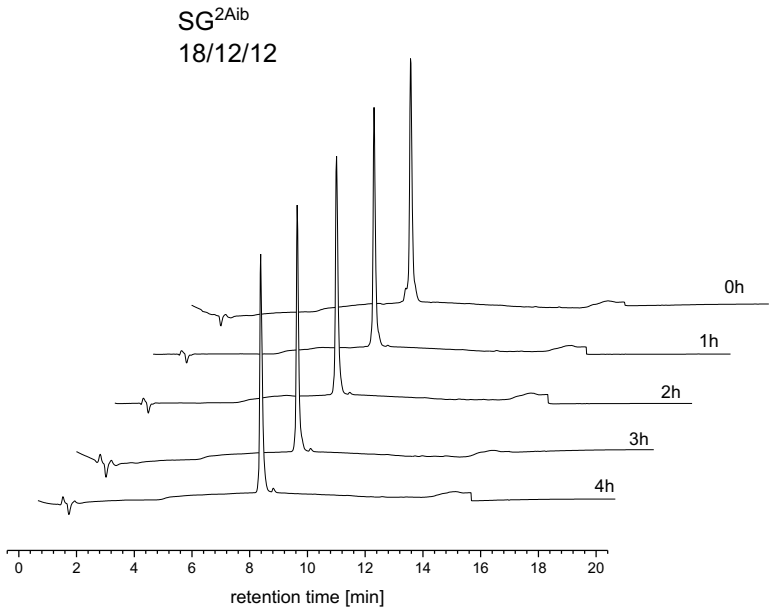

Figure S5 Chromatograms of enzymatic degradation after 1, 2, 3 and 4h with trypsin from peptide SG^{2Aib}.

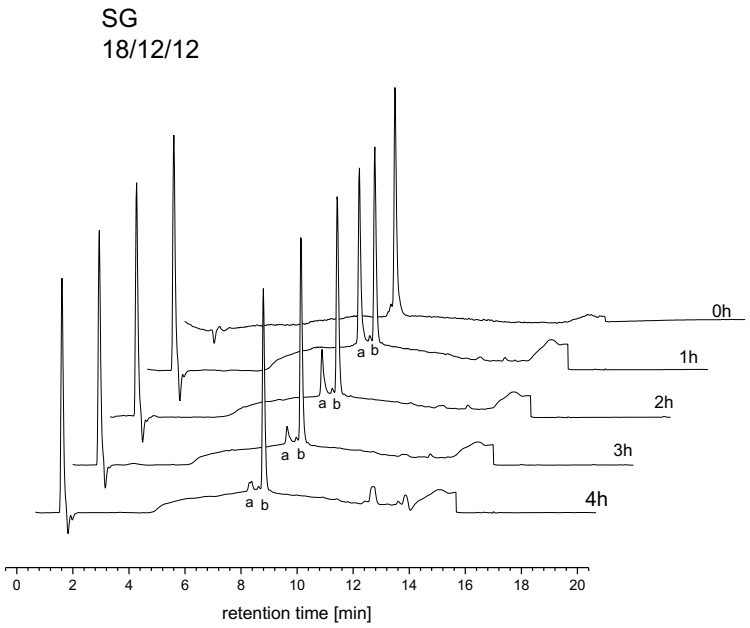

Figure S6 Chromatograms of enzymatic degradation after 1, 2, 3 and 4h with trypsin from peptide SG.

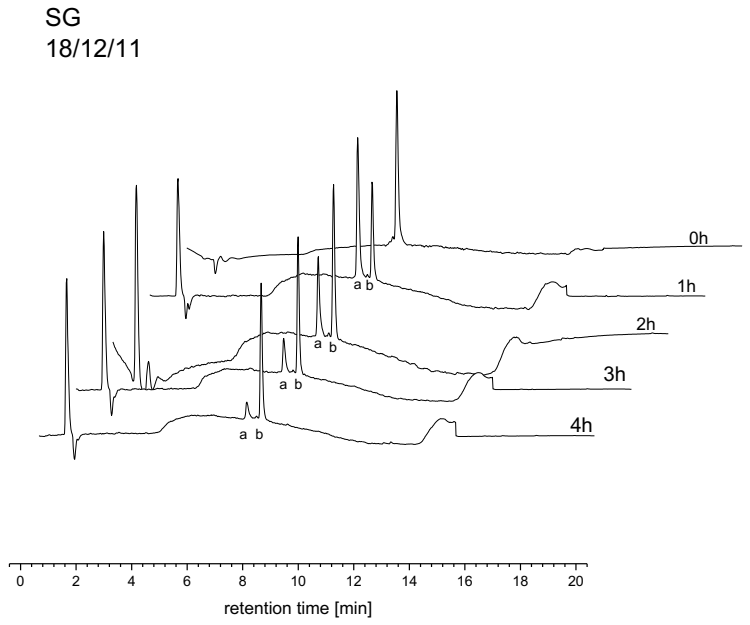

Figure S7 Chromatograms of enzymatic degradation after 1, 2, 3 and 4h with trypsin from peptide SG.

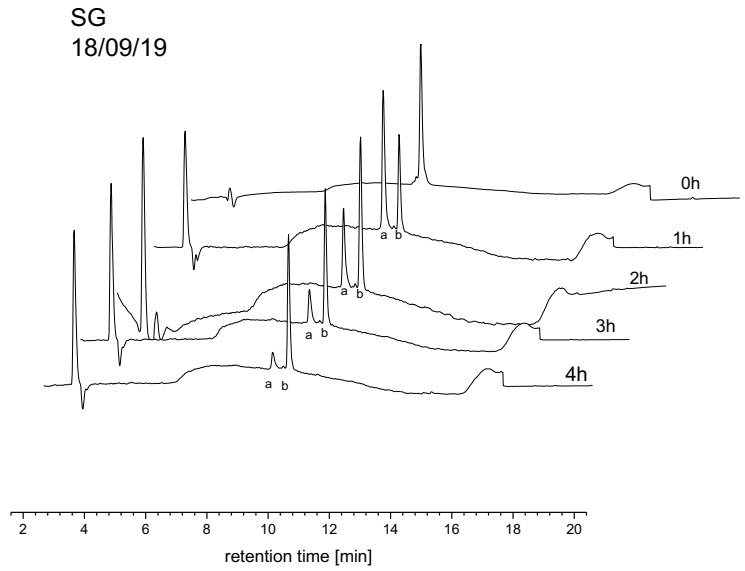

Figure S8 Chromatograms of enzymatic degradation after 1, 2, 3 and 4h with trypsin from peptide SG.

References

(1) Hornak, V.; Abel, R.; Okur, A.; Strockbine, B.; Roitberg, A.; Simmerling, C. *Proteins Struct. Funct. Bioinforma.* **2006**, *65* (3), 712–725. https://doi.org/10.1002/prot.21123.

(2) Lindorff-Larsen, K.; Piana, S.; Palmo, K.; Maragakis, P.; *Proteins Struct. Funct. Bioinforma.* **2010**, NA-NA. https://doi.org/10.1002/prot.22711.

(3) Wang, J.; Wolf, R. M.; Caldwell, J. W.; Kollman, P. A.; Case, D. A. *J. Comput. Chem.* **2004**, *25* (9), 1157–1174. https://doi.org/10.1002/jcc.20035.

(4) Jakalian, A.; Bush, B. L.; Jack, D. B.; Bayly, C. I. *J. Comput. Chem.* **2000**, *21* (2), 132–146. https://doi.org/10.1002/(SICI)1096-987X(20000130)21:2<132::AID-JCC5>3.0.CO;2-P.

(5) Jorgensen, W. L.; Chandrasekhar, J.; Madura, J. D.; Impey, R. W.; Klein, M. L. *J. Chem. Phys.* **1983**, *79* (2), 926–935. https://doi.org/10.1063/1.445869.

(6) Caleman, C.; van Maaren, P. J.; Hong, M.; Hub, J. S.; Costa, L. T.; van der Spoel, D. *J. Chem. Theory Comput.* **2012**, *8* (1), 61–74. https://doi.org/10.1021/ct200731v.

(7) Dupradeau, F.-Y.; Pigache, A.; Zaffran, T.; Savineau, C.; Lelong, R.; Grivel, N.; Lelong, D.; Rosanski, W.; Cieplak, P. *Phys. Chem. Chem. Phys.* **2010**, *12* (28), 7821. https://doi.org/10.1039/c0cp00111b.

(8) Bussi, G.; Donadio, D.; Parrinello, M. *J. Chem. Phys.* **2007**, *126* (1), 14101. https://doi.org/10.1063/1.2408420.

(9) Berendsen, H. J. C.; Postma, J. P. M.; van Gunsteren, W. F.; DiNola, A.; Haak, J. R. *J. Chem. Phys.* **1984**, *81* (8), 3684–3690. https://doi.org/10.1063/1.448118.

(10) Miyamoto, S.; Kollman, P. A. *J. Comput. Chem.* **1992**, *13* (8), 952–962. https://doi.org/10.1002/jcc.540130805.

(11) Hess, B. *J. Chem. Theory Comput.* **2008**, *4* (1), 116–122. https://doi.org/10.1021/ct700200b.

(12) Essmann, U.; Perera, L.; Berkowitz, M. L.; Darden, T.; Lee, H.; Pedersen, L. G. *J. Chem. Phys.* **1995**, *103* (19), 8577–8593. https://doi.org/10.1063/1.470117.

(13) Abraham, M. J.; Murtola, T.; Schulz, R.; Páll, S.; Smith, J. C.; Hess, B.; Lindahl, E. *SoftwareX* **2015**, *1–2*, 19–25. https://doi.org/10.1016/j.softx.2015.06.001.